

GAS HOLDUP IN A BENCH-SCALE DIRECT COAL LIQUEFACTION REACTOR

KIYOSHI IDOGAWA*, HIROSHI NAGAISHI,
HIDEO NARITA, TAKASHI FUKUDA,
TAKESHI KOTANIGAWA, RYOICHI YOSHIDA,
TADASHI YOSHIDA, SHINICHI YOKOYAMA,
MITUYOSHI YAMAMOTO, AKIYOSHI SASAKI,
MASAHIDE SASAKI, TOSHIMASA HIRAMA AND
YOSUKE MAEKAWA

Hokkaido National Industrial Research Institute, Sapporo 062

SHIGERU UEDA

New Energy and Ind. Tech. Dev. Organization, Tokyo 101

TADATOSHI CHIBA

Dept. of Metallurgical Eng., Hokkaido Univ., Sapporo 060

Key Words: Gas Holdup, Coal Liquefaction, High Pressure, High Temperature, Slurry Reactor, Gas Density, Liquid Density

Gas holdup was measured for gas-liquid (hydrogen gas/decrystallized anthracene oil/creosote oil) system and gas-slurry (hydrogen gas/Taiheiyo coal particles/decrystallized anthracene oil) systems in a 0.1 ton/day continuous direct coal liquefaction reactor. The measurements were carried out at temperatures ranging from 289K to 723K and a pressure of 30 MPa by two methods, a differential pressure method for the gas-liquid systems and a gas-quenching method for the gas-slurry system.

The gas holdups for both systems were correlated with the gas flow pattern just above the reactor entrance. Though the present gas holdup data were in reasonable agreement with those published by other investigators, a difference was found between the dependencies of gas holdup on superficial gas velocity in the preheater and in the reactor.

Introduction

For proper design of a chemical reactor and its operation it is vital to have sufficient knowledge about hydrodynamic behavior in the reactor as well as the reaction mechanism and rate. In particular, for two-phase and three-phase fluidized-bed reactors, gas holdup is one of the fundamental characteristics which governs the bulk flow pattern and the residence time distribution. The direct coal liquefaction system is a typical example of such reaction systems, consisting of hydrogen as the gas phase and coal and vehicle oil as the slurry phase. Normally, the system is operated at a temperature and pressure as high as about 720 K and 15 to 20 MPa respectively. The hydrogen gas holdup primarily affects the residence time distribution, which results in variations in coal conversion, product yield distribution and physical properties of the slurry phase. Therefore, it is very difficult to predict the flow behavior in the reactor directly from cold-model experiments. In addition, the variations in turn affect not only the design of operating variables to avoid residual solid accumulation in the reactor and to introduce quenching hydrogen gas into the reactor, but also the subsequent separation processes for gas-slurry and solid-product oils.

Mainly because of the difficulty in the operating experimental system and measurements under high-pressure and high-temperature conditions mentioned above, a very limited number of papers^{2, 5, 11, 12, 14, 16-20} have so far been published on the flow behavior in liquefaction reactors. Values of gas holdup have been often reported to be several times higher than those in air-water systems at room temperature and atmospheric pressure, even at the same volumetric gas velocity. This suggests that the flow in reactors tends to be a homogeneous bubbly flow^{18, 20, 21}, which would inevitably prevent rapid slurry mixing.

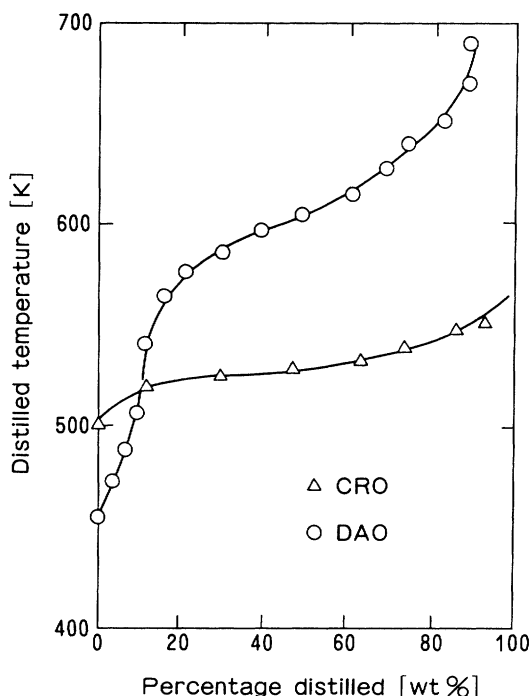
Once mixing becomes insufficient, an undesirable operating situation would occur, preventing the reactors from stable operation by forming dead space, a locally heated zone and a slurry lump or plug.

The present paper reports gas holdup data obtained by two methods, i.e., a differential-pressure method and a gas-quenching method, in a 0.1 ton/day continuous direct coal liquefaction reactor which has been operated in Hokkaido National Industrial Research Institute as a part of the Sunshine Project.

* Received May 26, 1993. Correspondence concerning this article should be addressed to K. Idogawa.

Table 1. Analysis of Taiheiyo Coal

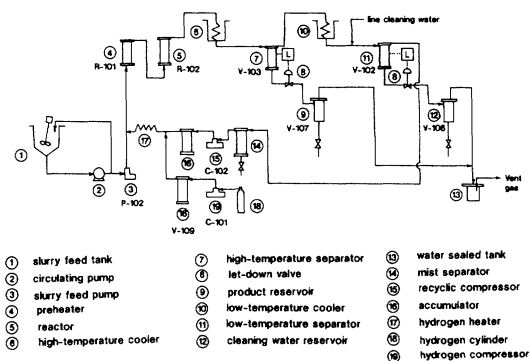
Proximate Analysis [Wt%, wet base]				
Moisture 5.90	Ash 12.55	Volatile Matter 44.64	Fixed Carbon 36.91	
Ultimate Analysis [Wt%, d.a.f. base]				
C 73.24	H 6.63	N 1.59	S 0.31	O 18.23

**Fig. 1** Distillation curves for creosote oil and decrystallized anthracene oil

1. Experimental

1.1 Materials

Particles used in the present experiments were Taiheiyo coal particles pulverized to under 100 mesh and dried at about 380 K until a constant weight was attained in an air stream under atmospheric pressure. Results of the proximate and the ultimate analysis of the coal are listed in **Table 1**. The coal particles were slurried with vehicle oil and fed to the reactor with catalyst particles and hydrogen gas. Gas holdups were measured in two kinds of systems: (1) non-reactive hydrogen gas-vehicle oil (gas-liquid) systems and (2) a reactive hydrogen gas-coal slurry (gas-slurry) system. In the former system, decrystallized anthracene oil (DAO) or creosote oil (CRO) was used as the liquid phase. Distillation curves of CRO and DAO are shown in **Fig. 1**. In the latter system, only DAO was employed as the vehicle oil and was mixed with coal particles at a weight ratio of 6 to 4 to form the slurry. Red mud crushed to under 100-mesh size together with elemental sulfur were added to the slurry as a catalyst and a sub-catalyst. Their weight ratios

**Fig. 2** Schematic flow diagram of 0.1 ton/day direct coal liquefaction process**Table 2.** Composition of the recycle gas

[wt%]							
H ₂	CH ₄	CO ₂	C ₂ H ₄	C ₂ H ₆	C ₃ H ₆	C ₃ H ₈	H ₂ S
99.42	0.051	0.416	0.016	0.038	0.034	0.008	0.02

to the raw coal particles were 0.05 and 0.005 respectively. The resultant density of the coal slurry was about 1240 kg/m³ under the present experimental conditions.

1.2 Apparatus

A schematic diagram of the 0.1 ton/day continuous direct coal liquefaction process is shown in **Fig. 2**. Coal slurry was fed into a preheater (4; R-101) by a slurry pump (3) from a slurry tank (1). The preheater had an inner diameter, D_i , of 4.0 cm and a height, H , of 100 cm. The slurry passed through the preheater then entered a reactor (5; R-102) with D_i of 8.0 cm and H of 100 cm. Hydrogen and recycle gases were supplied into the preheater through a gas heater (17) by a hydrogen compressor (19; C-101) and a recycle gas compressor (15; C-102), respectively. Recycle gas contained not only hydrogen gas but also those produced by coal liquefaction. A representative composition is shown in **Table 2**. The gases and the slurry were mixed before their entrance into R-101. The mixture was then fed to the reactor after being heated to a desired temperature in the preheater. The inner diameters of the injection nozzles of both R-101 and R-102 were 0.60 cm and their bottom shapes were of an inverse-conical type to promote dispersion of gas and liquid or slurry. The effluents from R-102 were separated into gas and liquid or slurry in the high-temperature separator (7; V-103), recycling the former as described above and storing the latter in a reservoir (9).

1.3 Methods of gas-holdup measurement

a) Differential pressure method

A differential-pressure method was employed for measurement of gas holdup in the reactor, with which a pressure-line system was connected as shown in **Fig. 3**. Three 4 mm i.d. tubes, A , B and C , were installed at the wall to detect the static pressure at three depths of 0, 20, and 80 cm from the bottom surface of the upper flange of

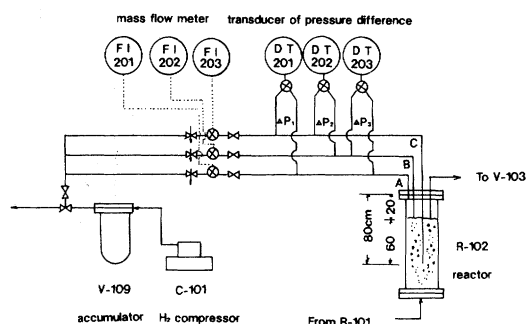


Fig. 3 Schematic diagram of system for differential-pressure measurement

the reactor. To prevent coke-blocking near the tips of the tubes, a steady hydrogen gas supply was maintained through each tube at a flow rate of about 280 Ncm³/s. This worked well for the gas-liquid systems. However, the gas supply was not effective for the gas-slurry system. The tips and the inside wall surfaces of the tubes were frequently blocked by fine solid particles of coal and catalyst and heavy coal-derived liquids, resulting in significant errors at the observed pressure.

The tip of the outlet tube was located at the same depth as tube B, i.e. 20 cm from the bottom surface of the upper flange, above which a stagnant gas phase was formed. Hence, in this method, the differential pressure measured between tubes A and B gives the gas density, ρ_g , while that between B and C gives the mean density, ρ , of mixture of the gas and the liquid phase. The density ρ_l of the liquid phase can further be determined by extrapolating the superficial gas velocity, u_g , to 0 cm/s. Once the densities, ρ , ρ_g and ρ_l are known, the gas holdup, ϵ_g , is calculated by the following equation:

$$\epsilon_g = (\rho_l - \rho) / (\rho_l - \rho_g) \quad (1)$$

b) Gas quenching method

For the gas-slurry system, gas holdups in the pre-heater (R-101) and in the reactor (R-102) were evaluated by a gas quenching method. Here, the reactor system was first settled at a steady state for a given temperature, pressure, gas and slurry flow rates. Then, the gas feeds from both the recycle and the hydrogen gas compressors (C-102 and C-101 respectively) into R-101 were shut off as quickly as possible while keeping the slurry supply at an unchanged rate. After the gas was quenched, all the gas bubbles in R-101 and R-102 disappeared within a measured time, leaving a slurry-free space which was gradually filled with the slurry fed successively. When the gas space was filled up, the slurry overflowed into the high-temperature gas-slurry separator, V-103 in Fig. 2. Responding to this, the slurry level in V-103 varied with time after the gas quench. The level first dropped quickly due to the effect of sudden gas quenching. Then, it remained constant for a while before the slurry overflowed from R-102. The level variation in V-103 was measured by a d.p. cell level meter.

Figure 4 demonstrates a typical variation of the

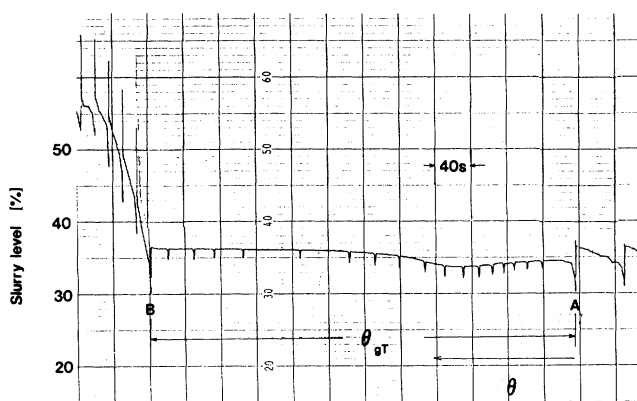


Fig. 4 Typical observed change of slurry level in V-103 with time after quenching gas:

$$Q_g = 5500 \text{ Ncm}^3/\text{s}$$

$$T_1 = 673 \text{ K}, T_2 = 723 \text{ K}$$

slurry level with time. It is clearly shown that the slurry level remains almost constant for the period θ_{gT} from A to B required for the slurry to replace the gas volume, $V_T \epsilon_{gT}$ left in R-101 and R-102 by the gas quenching. In this example, gas supply into R-101 was quenched at point A and the slurry overflow into V-103 commenced at point B. Though the variation is seen to be disturbed by irregular noise due to actuation of the pressure-regulated valve, it is not affected. From θ_{gT} for the constant level, the overall gas holdup, ϵ_{gT} , in R-101 and R-102 can be calculated by the following equation:

$$V_T \epsilon_{gT} = (W_{sl} / \rho_{sl}) \theta_{gT} \quad (2)$$

where W_{sl} and ρ_{sl} respectively represent the mass flow rate of slurry and slurry density. The gas holdup, ϵ_{g1} , in R-101 can be obtained by the same procedure as above by by-passing the effluents from R-101 to V-103 and consequently, ϵ_{g2} in R-102 can be given from the difference between ϵ_{gT} and ϵ_{g1} as

$$V_2 \epsilon_{g2} = V_T \epsilon_{gT} - V_1 \epsilon_{g1} \quad (3)$$

where V_1 and V_2 denote the volume of R-101 and that of R-102 respectively.

2. Results and Discussion

2.1 Gas-liquid systems

Figure 5 shows effects of the superficial gas velocity, u_g , on the gas density, ρ_g , at various temperatures and a pressure of 30 MPa. For both vehicle oils, CRO and DAO, ρ_g increased with temperature when u_g was smaller than 2 cm/s. When u_g exceeded 2 cm/s, values of ρ_g for both vehicle oils at different temperatures seemed to approach a value for the CRO-H₂ system at 473 K. The increase in ρ_g with temperature suggests that the light-oil fraction vaporizes more rapidly at higher temperatures and that the effect of temperature on vaporization is much more predominant than that on the hydrogen gas density, which decreases with increasing temperature. On the other hand, the vaporization was

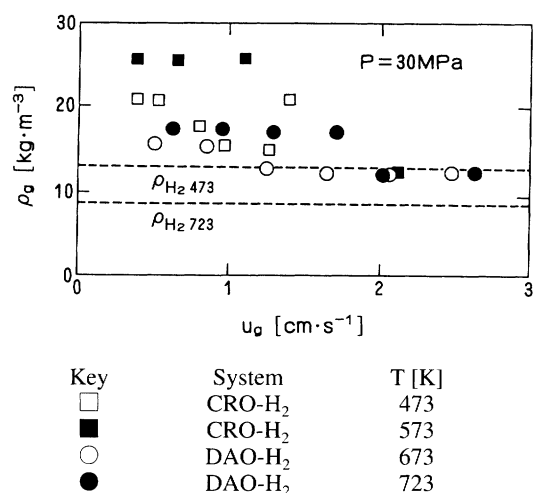


Fig. 5 Change of gas density with u_g for gas-liquid system

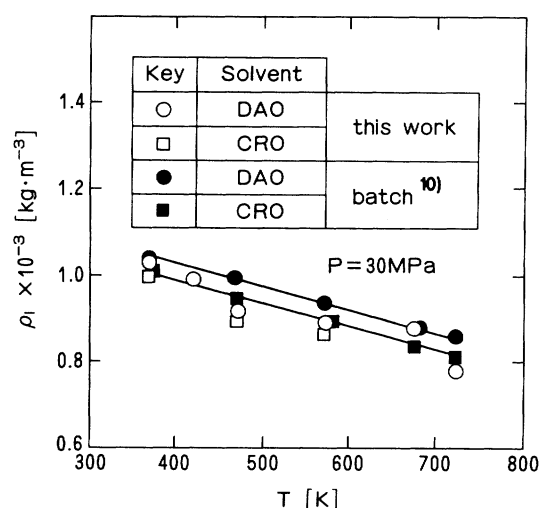


Fig. 6 Temperature dependency of liquid-phase density

suppressed as u_g increased because the residence time of slurry decreased with the increase of u_g , and this result led to a decrease of ρ_g with increase of u_g at higher temperatures. The temperature dependency of liquid density, ρ_l , when u_g was ρ_l to 3 cm/s and a pressure was 30 MPa, is shown in Fig. 6. Within the present operating conditions, no essential difference can be seen between the densities for CRO and DAO, and the present data agree well with those previously observed by the authors in a batch apparatus¹⁰⁾. In both the present and the batch¹⁰⁾ cases, ρ_l decreased linearly with temperature.

Based on the density change in ρ_g and ρ_l mentioned above, values of the gas holdup, ϵ_g , in R-102 were calculated by Eq. (1). The result is shown in Fig. 7. Although the calculated data scatter a little widely, the values of ϵ_g seem to be almost independent of temperature and kind of vehicle oil, and increase with the increase of u_g . It should be noted that the values of ϵ_g are higher than twice those observed by Akita and Yoshida¹⁾ for an air-water system at room temperature and atmospheric pressure. While they separately supplied gas and liquid at atmospheric pressure, pressurized gas and liquid

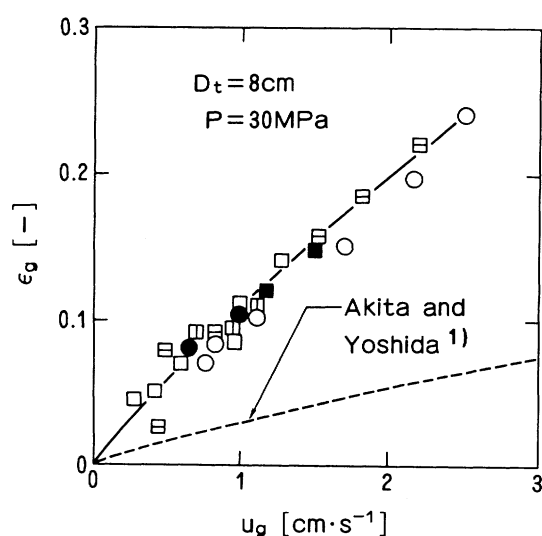


Fig. 7 Effects of superficial gas velocity and temperature on gas holdup in gas-liquid system

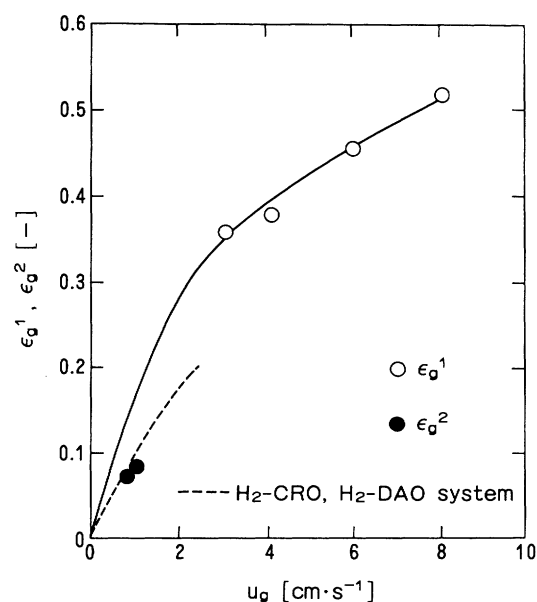


Fig. 8 Comparison of gas holdups in preheater (R-101) and reactor (R-102)

were simultaneously supplied into the reactor in the present experiments. According to our previous photographic observations⁶⁻⁸⁾, high pressure in the former case causes size reduction of generated bubbles due to the increase in kinetic energy. In addition to size reduction, the simultaneous gas-liquid supply at high pressure also causes the formation of an active jet, at the nose and the circumference of the nozzle from which tiny bubbles are generated⁹⁾. The bubbles ascended through the liquid phase as a swarm with less frequent coalescence than in

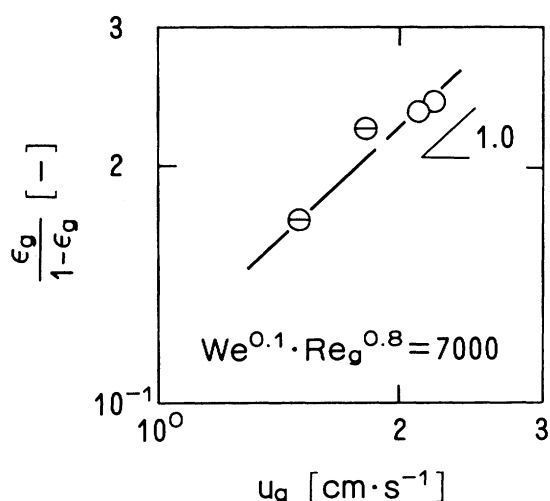


Fig. 9 Effect of u_g on $\epsilon_g/(1 - \epsilon_g)$ at $We^{0.1} Re_g^{0.8} = 7000$; keys are listed in Table 3

Table 3. Experimental conditions and keys for Figs. 9 to 12

Key	D_i [cm]	d_N [mm]	T [K]	P [MPa]	u_i [cm/s]	Liquid	Method	Authors
⊖	8	6	289-573	30	0.05	CRO	DP	present authors
○	8	6	673, 723	30	0.05	DAO	DP	
●	8	6	723	30	0.05	slurry	QM	
⊙	8	6	373-573	30	0.05	CRO	QM	
⊕	8	6	673	30	0.05	DAO	QM	
△	13	15	473-654	5-17.4	0.25	recycle solvent	QM	Hayakawa ⁵⁾
▢	24	18.7	301-323	13-23.5	0.17	CRO	DP	Mochida ⁴⁾
□	24	18.7	573	23.5	0.17	DAO	DP	
▽	6.6		700-722	13.6-17	0.55	slurry	RT	Tarmy, et al. ^{18, 19)}
▽	61		700-722	13.6-17	1.65	slurry	RT	
◇	120		753	31		slurry		Kürten ¹¹⁾

DP: differential pressure; QM: gas quenching; RT: radioactive tracer

atmospheric air-water systems.

2.2 Gas-slurry system

Gas holdup in the gas-slurry system was measured at 30 MPa and temperatures in the preheater (R-101) and in the reactor (R-102) of 673 K and 723 K. Fig. 8 shows the variation with superficial gas velocity, u_g , of the gas holdup, ϵ_{g1} , in R-101 and ϵ_{g2} in R-102. In the present experiments, u_g in R-101 was always higher than that in R-102 at a given flow rate. Hence, as shown in the figure, ϵ_{g1} was always greater than ϵ_{g2} . However, the values of ϵ_{g1} seem to be unusually high compared with those in air-water systems at room temperature. As mentioned above, it seems to produce smaller-size bubbles to simultaneously supply pressurized gas and liquid. In addition, the slurry viscosity in R-101 seems to increase with the progress of volumetric swelling of coal particles and the accumulation of heavy-oil products on the surface of coal particles, both of which make the mean slurry viscosity in R-101 much higher than the viscosity

Table 4. Physical properties of gas and liquids assumed for calculation of $We^{0.1} Re_g^{0.8}$

Fluid	T [K]	P [MPa]	gas density $\rho_g^{a)}$ [kg/m ³]	gas viscosity $\mu_g \times 10^{7b)}$ [Pa·s]	surface tension $\sigma \times 10^{3c)}$ [N/m]	liquid density $\rho_l^{d)}$ [kg/m ³]
CRO	289	30	11	90	36	1070
CRO	373	30	13	100	33	995
CRO	473	30	16	123	28	940
CRO	573	30	20	140	20	880
DAO	673	30	15	157	13	870
DAO	723	30	18	165	11	855
slurry	723	30	103	165	11	770

a) observed values for CRO and DAO and estimated value for slurry from Lin et al.¹³⁾

b) estimated from Perry¹⁵⁾

c) estimated from Gray and Holder⁴⁾

d) observed values¹⁰⁾

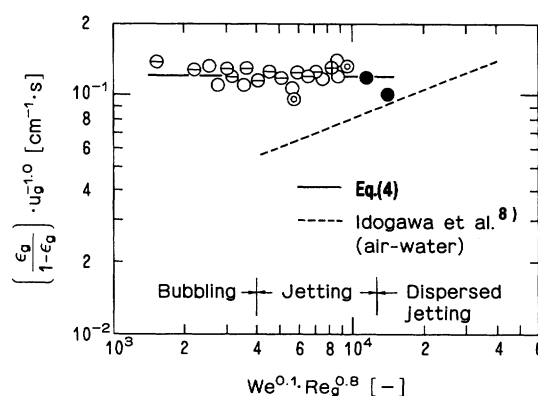


Fig. 10 Correlation of $\epsilon_g/(1 - \epsilon_g) u_g^{-1}$ with $We^{0.1} Re_g^{0.8}$; keys are listed in Table 3

of water³⁾ at room temperature. The high slurry viscosity in turn reduces the initial bubble size and the ascending velocity of bubbles, and all of these effects contribute to the unusually high values of ϵ_{g1} . In contrast to ϵ_{g1} , the observed gas holdup, ϵ_{g2} , in R-102 is in good agreement with values for the gas-liquid systems shown by a broken line in the figure, since the slurry viscosity in R-102 would be as low as that of the coal liquids, CRO and DAO, due to the progress of the liquefaction reaction.

According to our previous experimental work regarding gas holdup, ϵ_g , in a high-pressure bubble column with a single orifice⁸⁾, ϵ_g was found to be closely related to the pattern of bubble formation above the distributor which is characterized by a term of dimensionless numbers, $We^{0.1} Re_g^{0.8}$. Here, the term was applied to the analysis of the present gas holdup data. For a jet formation regime with $We^{0.1} Re_g^{0.8} = 7000$, the relationship between $\epsilon_g/(1 - \epsilon_g)$ and u_g is shown in Fig. 9, where the keys and experimental conditions are listed in Table 3 and the physical properties necessary for the calculation of We and Re_g numbers are in Table 4. It is clearly indicated in the figure that the holdup ratio increases in proportion to u_g . The values of $\{\epsilon_g/(1 - \epsilon_g)\} u_g^{-1}$ are plotted against $We^{0.1} Re_g^{0.8}$ in Fig. 10, but they seem to be substantially independent of the dimensionless term regard-

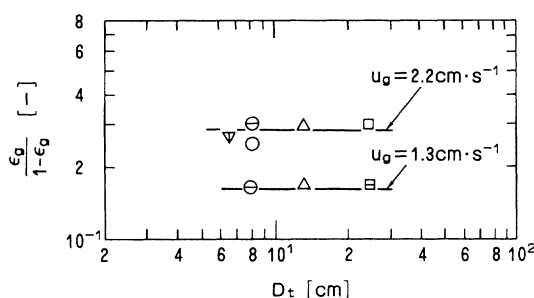


Fig. 11 Effect of reactor diameter on $\varepsilon_g / (1 - \varepsilon_g)$; keys are listed in Table 3

less of the flow pattern, i.e. the bubbling or jetting regime, and they are correlated by the following equation:

$$\varepsilon_g / (1 - \varepsilon_g) = 0.12 u_g \quad (4)$$

The above correlation differs from that for an air-water system⁸⁾ (the broken line in the figure) which is expressed as

$$\varepsilon_g / (1 - \varepsilon_g) = 0.005 u_g^{0.7} (We^{0.1} Re_g^{0.8})^{0.3} \quad (5)$$

A possible explanation for the difference is as follows. In the air-water system the bulk bubble flow and coalescence between bubbles were affected by the pattern of bubble formation above the gas distributor with a single orifice, and the bubbles grew in size by coalescence. In the present systems, on the contrary, the initial bubble sizes were so small that they exhibited neither detectable dependency on bubble formation patterns as shown in the figure nor bubble growth comparable to that in the air-water system. In **Fig. 11** the present data on ε_g in the reactor are compared with those published by other investigators for different reactor diameters, D_t . As can be seen, the gas holdup does not depend on D_t at a given u_g , again suggesting that the flow in coal liquefaction reactors tends to be in a homogeneous bubbly flow regime.

All the data obtained from experiments listed in Table 3 are summarized in **Fig. 12** on the basis of Eq. (4). It is noted that the gas holdups in the coal liquefaction reactors with D_t in a range of 6.5 to 120 cm can be correlated by the equation within an accuracy of $\pm 50\%$ in spite of rather different experimental conditions and methods of measurement.

Conclusions

From measurements of gas holdup in a 0.1 ton/day direct coal liquefaction reactor the following points are concluded within the present experimental conditions.

- 1) The gas flow pattern in the reactor was found to be a homogeneous bubbly flow.
- 2) The gas holdup in the reactor was almost independent of the pattern of bubble formation. This seems to be the result of the tiny initial size of bubbles formed by

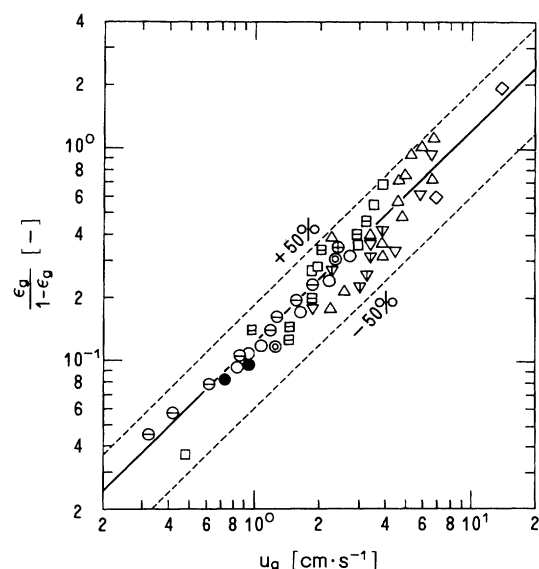


Fig. 12 Comparison of gas holdups from present experiments with those in literature; keys are listed in Table 3

the simultaneous supply of pressurized gas and liquid from the injection nozzle of the reactor as well as the suppressed bubble growth.

- 3) The gas holdup was also found to be independent of reactor diameter from the same reason as above and was well correlated by Eq. (4) with the superficial gas velocity.

In a coal liquefaction reactor, steady operation could be realized by suppressing the accumulation of residual solid and promoting heat transfer and dispersion of quenching hydrogen gas introduced, which are secured by vigorous mixing of solid or slurry. It would therefore be necessary to produce a moderate turbulent flow in the reactor. However, the present experimental results clearly suggest that the flow tends to be reduced to undesired homogeneous bubbly flow. Further work is necessary to find proper operating conditions for transition of the flow regime.

Acknowledgment

The authors are very grateful to Dr. S.L. Jimmy Yun (HNIRI) and Mr. K. Hayakawa (Sumitomo Metal Co., Ltd.) for their useful comments and discussions.

Nomenclature

D_t	= diameter of reactor	[m]
d_N	= diameter of nozzle	[m]
H	= height of reactor	[m]
P	= pressure	[MPa]
Q_g	= volumetric gas flow rate at normal state	[Nm ³ /s]
Re_g	= gas-phase Reynolds number based on nozzle diameter ($= d_N u_N \rho_g / \mu_g$)	[-]
T	= temperature	[K]
u_g	= superficial gas velocity at experimental conditions	[m/s]
u_l	= superficial liquid velocity at experimental conditions	[m/s]
u_N	= gas velocity through nozzle at experimental conditions	[m/s]

V	= volume of reactor	[m ³]
We	= Weber number ($\rho_f d_N u_N^2 / \sigma$)	[-]
W_{sl}	= mass flow rate of slurry	[kg/s]
ϵ	= holdup	[-]
μ	= viscosity	[Pa·s]
ρ	= density	[kg/m ³]
θ	= time	[s]
θ_g	= time required to replace gas in reactor with slurry	[s]
σ	= surface tension of liquid	[N/m]

<Subscripts>

1	= preheater
2	= reactor
g	= gas
l	= liquid
sl	= slurry
T	= preheater + reactor

Literature cited

- 1) Akita, K. and F. Yoshida: *Ind. Eng. Chem. Process Des. Dev.*, **12**, 76-80 (1973)
- 2) Deckwer, W.D., Y. Loisi, A. Zaidi and M. Ralek: *ibid*, **19**, 699-708 (1980)
- 3) Deng, C.-R., T. Nio, Y. Sanada and T. Chiba: *Fuel*, **68**, 1134-1139 (1989)
- 4) Gray, J.A. and G.D. Holder: DOE/ET/10104-44, April (1982)
- 5) Hayakawa, K: personal communication on the gas holdup in a 1-ton/day direct coal liquefaction reactor (Sumitomo Metal Co.), (1991)
- 6) Idogawa, K., K. Ikeda, T. Fukuda and S. Morooka: *Kagaku Kogaku Ronbunshu*, **11**, 432-437 (1985)
- 7) idem: *ibid*, **12**, 107-109 (1986)
- 8) idem: *Chem Eng. Commn.*, **59**, 201-212 (1987)
- 9) Idogawa, K., T. Fukuda, H. Nagaishi, Y. Maekawa, T. Chiba and S. Morooka: *Kagaku Kogaku Ronbunshu*, **16**, 1210-1216 (1990)
- 10) Idogawa, K., T. Fukuda, A. Sasaki, H. Nagaishi, T. Kotanigawa and T. Chiba: Preprint of Muroran Meeting of the Soc. of Chem. Engrs., Japan, No. B-105, Muroran (1992)
- 11) Kürten, H.: *Chem. Ing. Tech.*, **54**, 409-415 (1982)
- 12) Lee, K.K., R.W. Hawkins, H. Narita, Y. Maekawa and A. Hardin: Proc. of Int. Conference on Coal Science, Vol.II, p. 863 Tokyo (1989)
- 13) Lin, H.M., W.A. Leet, H. Kim and K.C. Chao: *Ind. Eng. Chem. Process Des. Dev.*, **24**, 1225-1230 (1985)
- 14) Mochida, N.: "Direct Coal Liquefaction", Presented at Chemical Plant Engineering Conference, Tokyo (1985)
- 15) Perry, R.H.: "Chemical Engineers Handbook", 3rd ed. (1950)
- 16) Rundel, D.N. and R.J. Schefer: *Ind. Eng. Chem. Res.*, **26**, 613-617 (1987)
- 17) Sangnimnuan, A., G.N. Prasad and J. Sgnew: *Chem. Eng. Commun.*, **25**, 193-212 (1984)
- 18) Tarmy, B., M. Chang, C. Coulaloglou and P. Ponzi: *The Chem. Engr.*, 18 (Oct. 1984)
- 19) idem: Chem. Eng. Symp. Series, No. 87, 303-317 (1984)
- 20) Yamaguchi, H., T. Ogawa and T. Yokoyama: *Nenriyo Kiyokaishi*, **70**, 1143-1150 (1991)